Strojnícky časopis – *Journal of* MECHANICAL ENGINEERING,
VOL 74 (2024), NO 3, 105 - 120

FATIGUE EXPERIMENTAL OF AS-CAST Ti-6Al-7Nb IMPLEMENTED ON DESIGNED FEMORAL STEM FOR INDONESIAN PEOPLE THROUGH FINITE ELEMENT ANALYSIS

GALIH Taqwatomo[1*], AGHNI Ulma Saudi[2], DAMISIH[2], NANDANG Suhendra[2], MIRZA Wibisono[2], GIRI Wahyu Alam[2], I NYOMAN Jujur[2], WINDA Rianti[2], SITI Amalina Azahra[2], MUHAMMAD Dikdik Gumelar[1], DITA Adi Saputra[1], SADDAM Husin[1], RIASTUTI Fidyaningsih[2]

[1] *Organization Research of Energy and Manufacture, National Research and Innovation Agency (BRIN), B.J. Habibie Science and Technology Area, South Tangerang, Banten 15314, Indonesia,*
e – mail: gali011@brin.go.id
[2] *Organization Research Nanotechnology and Material, National Research and Innovation Agency (BRIN), B.J. Habibie Science and Technology Area, South Tangerang, Banten 15314, Indonesia*

Abstract: This study aims to evaluate the durability of as-cast Ti-6Al-7Nb in femoral stem application using fatigue analysis. As-cast Ti-6Al-7Nb rod specimens were tested experimentally with load range of 120%, 100%, 90%, 80%, 70%, 50%, 30%, and 20% relative to the yield strength. The fatigue limit was identified on a range of 141 - 211 MPa, represented by two run-out specimens running until high fatigue cycle (HFC) of 10^7 without failure. ProFatigue contributed to expose the estimation of the expected failure cycle on fatigue limit stress of as-cast Ti-6Al-7Nb based on Weibull modelling. It was predicted by probability failure (P_{fail}) of 50%. The failure cycles were revealed at 2.144 x 10^7 and 2.823 x 10^9 cycles on amplitude stress of 211 and 141 MPa, respectively. The reliability of the designed femoral stem for Indonesian people has been analyzed under ISO 7206 configuration through finite element analysis by adopting the material properties of as-cast Ti-6Al-7Nb. The static linear analysis demonstrated the maximum stress concentration of 136 MPa occurring over the medial region of the femoral stem, showing lower stress levels compared to the fatigue limit of as-cast Ti-6Al-7Nb. Furthermore, the lifetime analysis computed that the design could withstand cyclic loading until 2.51 x 10^9 cycles with fatigue safety factor and damage factor in 1.763 and 0.398, respectively. Results concluded that the investment casting is evident to become an alternative manufacturing method of femoral stem made of Ti-6Al-7Nb.

KEYWORDS: Experimental fatigue, Pro-Fatigue, FEA

1 Introduction

The enormous growth of citizen in Indonesia leads to the enhancement of health services as well as the technology supporting the healthcare [1]. Biomaterials play an important role in improving the quality of human life, especially for those who are in the elderly group, as they often encounter some complications in their musculoskeletal as well as their bone health [2,3]. Total hip arthroplasty (THA), is one the most common orthopedic implants that are used as hip joint prostheses for patients suffering from degenerative, accidents, hip osteoarthritis, hip osteonecrosis, and other medical conditions [4].

Titanium alloy is still one of the best options for biomedical implant application, thanks to its superior mechanical properties, high strength-to-weight ratio, and exceptional surface characteristic, which is responsible for its corrosion and wear resistance [5,6]. Researchers have been developing a titanium alloy known as Ti-6Al-4V that incorporates vanadium for use in medical devices like dental implants and orthopedic prostheses [7]. However, the vanadium ion in this particular alloy may become toxic to human tissue after long-term use. As a result, a

DOI: 10.2478/scjme-2024-0038, Print ISSN 0039-2472, On-line ISSN 2450-5471

new, safer, and non-hazardous alloy called Ti-6Al-7Nb has been introduced as a replacement for Ti-6Al-4V [8]. A large study of mechanical properties, castability, and wear characteristics of Ti-6Al-7Nb casting alloy have been observed comprehensively [9-12]. Conversely, investigation regarding fatigue behavior of as-cast Ti-6Al-7Nb revealed limitedly. In addition, examining the exact number of failure cycles on fatigue limit is an ongoing challenge in experimental fatigue studies. It was limited by equipment capacity and needed long-time research to run the very high cycle fatigue (VHCF) to expose it [12,13].

The study aims to reveal the S-N curve of as-cast Ti-6Al-7Nb experimentally, then expose the estimation of the maximum failure cycle on the fatigue limit stress based on probabilistic modelling using the ProFatigue program. The entire material properties of as-cast Ti-6Al-7Nb were applied to the designed femoral stem for Indonesian people in order to evaluate the endurance of design through the finite element method according to ISO 7206 standards.

2 Material and Method

2.1 Experimental Fatigue Test

Wrought Ti-6Al-7Nb alloy (ASTM F 1295, Daido Steel, Japan) was melted in a vacuum electric arc furnace and poured into the cylindrical shape ceramic-based mold. The chemical composition is C: 0.01, Al: 6.13, Nb: 7.4, O: 0.18, N: 0.01, Fe: 0.2, Ta: <0.01, Ti balance. The as-cast Ti-6Al-7Nb alloy was then machined into fatigue specimens form, according to ASTM E 466.

Table 1. The average mechanical properties of the as-cast Ti-6Al-7Nb.

Parameters	**Value**
Elongation (%)	9.8
Young’s modulus (GPa)	101.7
Poisson ratio	0.36
UTS (MPa)	888
Yield Strength (MPa)	706
Hardness (HV)	385

Specimens were then subjected to fatigue using a dynamic testing machine (Hung Ta, Taiwan, HT-9711 T5) to form an S-N curve and ascertain the fatigue strength of the as-cast Ti-6Al-7Nb in a specimen level before upscaling it to a product level. The load’s range used is 120%, 100%, 90%, 80%, 70%, 50%, 30%, and 20%, to the yield strength shown in Table 1. Tensile tests were carried out on 5 specimens of the as-cast Ti-6Al-7Nb according to the ASTM E8; the summary of the tensile test was presented in Figure 1.

Figure 2 shows the detailed dimension of fatigue specimens with a center diameter modified to 2.5 mm to obtain the desired stress adapted to the fatigue equipment's limit on the maximum load of 5 kN. 10 Hz was used as the test frequency and symmetrical loading with tension-compression R= -1 with maximum cycles set at 107 per fatigue test in air. When the specimen breaks before reaching the maximum cycle, the dynamic loading will automatically stop and the failure cycles going to be logged

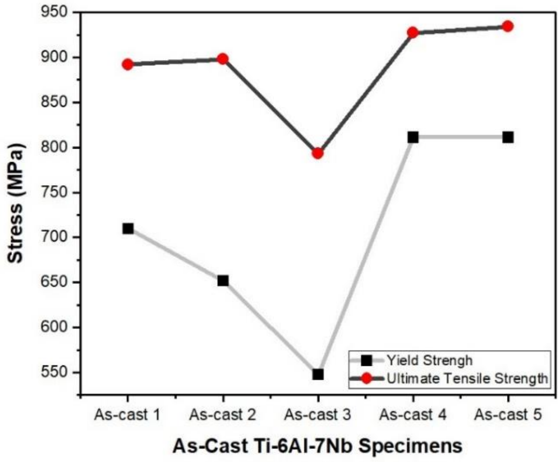

Fig 1. Summary of tensile test on 5 specimens as-cast Ti-6Al-7Nb.

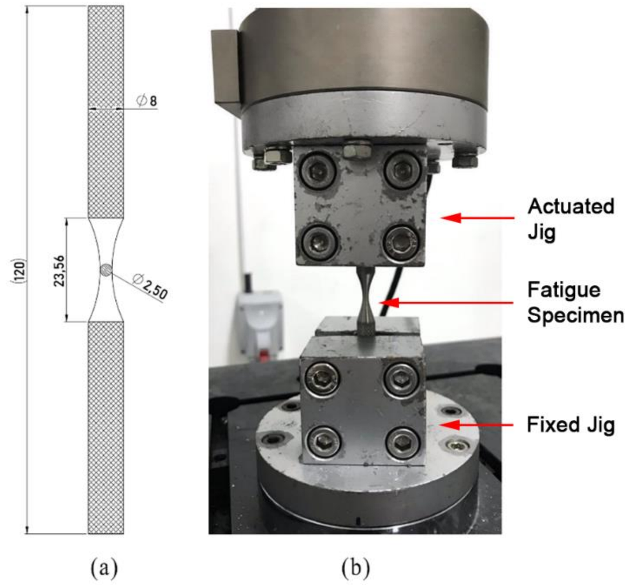

Fig 2. Fatigue specimens Ti-6Al-7Nb as-cast (a) detail dimension and (b) installation fixture test.

2.2 Pro-Fatigue Software

ProFatigue program was a free-use software to facilitate the prediction of the fatigue cycles materials based on the probabilistic model by inputting the experimental data, proposed by Castillo-Canteli [14]. The program accommodates the Weibull and the Gumbel parameters to calculate of the fatigue data [15]. The following study, only based on the Weibull model distribution as given in Eq.(1) and Eq.(2), defines the S-N or ε-N fields as hyperbolic curves through a comparable failure probability [16].

$$P_f(N, \Delta\sigma) = 1 - \exp\left[-\left(\frac{V - \lambda}{\delta}\right)^{\beta}\right] \quad (1)$$

where,

$$V = (logN - B)(log\Delta\sigma - C); V \geq \lambda \quad (2)$$

The equation shows P_{fail} represents the probability of failure, N is the number of cycles, V is the normalized variable, β, λ, δ represent shape, location and scale parameters, respectively.

B shows the threshold for lifetime and C performs the endurance fatigue limit as the threshold parameter for stress level [17].

The corroboration of reliability and capability of the Weibull probabilistic distribution on ProFatigue software has been presented in a broad range of research studies as reported on [12,15,18]. All of the research studies have revealed potential advantages of ProFatigue software enforced in fatigue research, including:

The potential to perform efficient fatigue experimental planning is by reducing the total amount of tests planned. The S-N analytic expression has immediate implications in that the calculation is able to estimate the number of cycles for a certain specific stress range and probability, or instead based on the regression result of experimental data statistics [15]. In most circumstances, 8-10 specimens would be enough to provide a reliable assessment of the S-N fields as long as conducting the load ranges is distributed appropriately [19]. Thus, it is not essential to repeat the tests under the identical load range to complete the statistical analysis. Conversely, to ISO Standard procedure required carrying out multiple tests for the exact same load range as validation to determine the S- N field [15].

The software application supports taking into account the assessment parameter of the impact of run-out specimens, it means non-failed test that usually occurs on the low load range of fatigue test [17]. Researchers typically specify a predetermined number of cycles, commonly 2, 5 or 10 million, which is incorrectly considered as the material fatigue limit with an infinite number of cycles [20]. Therefore, it must be assumed that the fatigue test to achieve the fatigue limit material experimentally required a high number of cycles due to the specimens failing is unknown. The software features a sophisticated mathematical extrapolation technique enabling a considerably more stringent and accurate comparative examination to produce a more precise definition of the accurate fatigue limit for each run- out specimen [15].

In this study, ProFatigue software applied the Weibull regression model to optimize the experimental fatigue on run-out specimens of the as-cast Ti-6Al-7Nb. Once probabilistic modeling is generated, it exposes an estimation limit of the failure cycle for the run-out specimens and correspondently be applied to the S-N curve properties for the finite element analysis.

2.3 Finite Element Analysis

Geometry Model

The geometric design of the femoral stem was a recent study development by modifying the commercial product with the recommended dimensions adapted to Indonesian femur bone [21,22]. CAD model shown in Figure 3(a) with the dimensions of the total length, thickness and angle neck of the femoral stem are 145 mm, 10 mm and 135°, respectively. In addition, the mediolateral dimensions are width-1: 30,66 mm, width-2: 15,95 mm, and width-3: 8,29 mm. Then, the outer curvature diameter of the femoral head was 26 mm. The femoral neck design refers to a modular 12/14 taper profile with tolerance ± 0,05 mm to maintain the precision lock assembly with the inner tapper of the femoral head [23]. In order to evaluate the endurance performance of this femoral stem design, the configuration test of ISO 7206 was applied to simulate the fatigue test for the designed femoral stem through finite element analysis.

Solid model parts were produced by the integration of extrude boss, extrude cut, revolve, and lofted techniques using Solidworks software. Those CAD models were initially created separately as solid components in part features. Then, all solid parts were connected utilizing the assembly feature to create an accurate configuration shown in Figure 3(b). The measured dimension from the endpoint stem to the center of the femoral head (CT) is 148 mm; according to ISO 7206, the femoral stem design is classified into 120>CT>200 mm category fatigue test. Thus, offset distances from the top surface of bone cement into the center of the femoral head (D) must be 80 mm, angle of femoral stem β and α are 9°, 10° respectively [24].

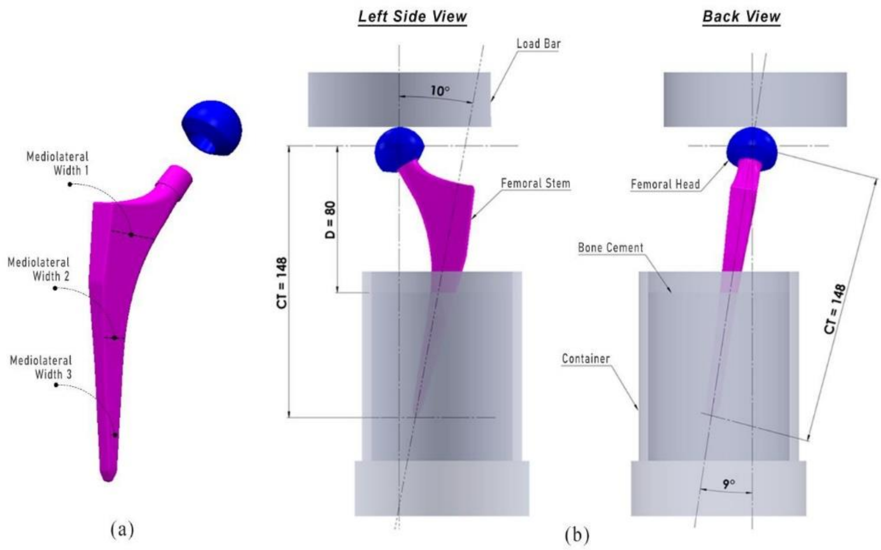

Fig 3. (a) CAD part model of recent study modified design of femoral stem for Indonesia patients, (b) CAD Assembly model according to ISO 7206 configuration fatigue test.

The plane and surface of components were utilized to be a tool reference for positioning a femoral stem appropriate with the regulation of ISO 7206. The assembly model has been evaluated by interference detection for ensuring there are no errors in surface interaction that causes issues and inaccuracy in finite element solutions.

Pre-Processing FEA

The durability of the design implant investigated through finite element (FE) analysis based on mathematical computational methods by geometric discretization of FE models into smaller and simpler elements [25,26]. The three-dimensional assembly femoral stem ISO 7206 was imported from Solidworks into the ANSYS workbench within Parasolid (x.t) format type. The mesh method setting is applied to all body models employing tetrahedrons with matrix-type elements of SOLID 187, CONTA 174 and TARGE170, which have adaptive mesh to geometric irregularities.

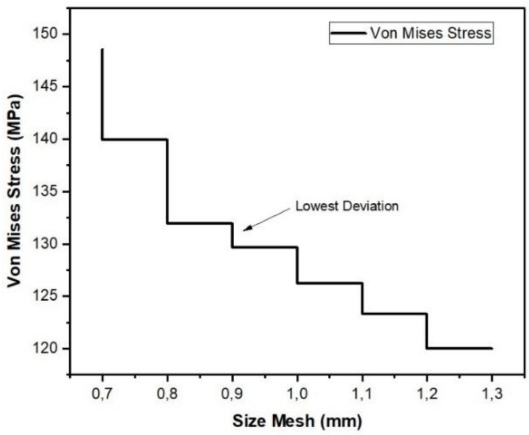

Fig 4. Convergence analysis of size mesh for finite element model fatigue femoral stem.

Different sizing meshes are applied to the FE model to improve the efficient running time of the FE solution. Coarse meshing enforced to the models of load bar, container and bone cement with a size mesh of 5 mm. Meanwhile, fine meshing was applied to the model of femoral head and stem with a variety of size mesh, 0.7, 0.8, 0.9, 1, 1.1, 1.2 and 1.3 mm, which aimed to define the most stable mesh by comparing the result of von mises stress on each size mesh through convergences analysis shown in Figure 4. The maximum stresses emerge on the same location elements on the femoral stem model with fluctuating values depending on the characteristic of each size mesh. As a result, a size mesh 0.9 mm was selected due to exhibiting the lowest deviation result among others. The assembly FE model consists of approximately 898,000 elements and 1,200,000 nodes. The meshed FE model is present in Figure 5(a).

A variety of material properties for the FE model have been selected following ISO 7206. The femoral stem used mechanical properties corresponding to the experimental study of as-cast Ti-6Al-7Nb present on Tabel 1. In addition, the femoral head, load bar, container and bone cement are applied materials of CoCr, stainless steel and bone cement, respectively. The detail specifications of mechanical properties presented in Table 2. Those material properties are assumed to be homogeneous linear isotropic behavior.

Table 2. Material properties for femoral head, fixture (load bar & container) and bone cement on FEM.

Material Description	Young's modulus (Gpa)	Poisson ratio
CoCr [27]	220	0.33
Bone cement [28]	2.3	0.33
Stainless steel [29]	205	0.3

The contact interaction applied in different types on FE models is displayed in Table 3. Jonathan et al. have demonstrated the result of finite element on cemented hip arthroplasty given more damage prediction by utilizing the non-linear contact [30]. In this study, the friction coefficient assumed 0.2 as an average value of friction factor [31]. In other places, linear contact or bonded type were implemented to illustrate the adhesion condition.

Table 3. Type of contact for femoral head, fixture (load bar & container) and bone cement component on boundary condition.

Contact interaction		Type of contact
Contact body	Target body	
Femoral head	Load bar	Nonlinear – frictional, CoF 0.2
Femoral stem	Femoral head	Nonlinear – frictional, CoF 0.2
Femoral stem	Bone cement	Nonlinear – frictional, CoF 0.2
Bone cement	Container	Linear - bonded

The loading conditions for the FE model have been set up to be compliant with the configuration described in ISO 7206, as shown in Figure 5(b). The axial force in the -y direction was inserted at the bottom surface of the load bar at 2300 N. In addition, a displacement setting was adopted around the surface of the load bar to maintain the acti component only moving in the -y axis direction. The location of fixed support is defined at the bottom surface of the container. To create the gravitational influence on the -y direction, the standard earth gravitational parameter was added to the loading condition.

In this study, finite elements were divided into two-step; First, finite element models are computing on the linear static which activates the large deformation setting to observe realistically the distribution of equivalent stress and displacement elements focused on the femoral stem mode [32]. The solution visualizes on failure evaluation of von mises stress, maximum principal stress, minimum principal stress and total deformation. Then, the linear static solution subsequently be inputted into the fatigue tool analysis. The program could estimate the femoral stem's lifetime with an extrapolation method based on log-log calculation, comparing the von-mises stress results to the S-N data of Ti-6Al-7Nb as-cast [33]. The loading condition would improve into sinusoidal constant amplitude with proportional loading R=0.1, with force maximum -2300 N and minimum -230 N. Fatigue empirical relations of Goodman, Gerber, Soderberg, and ASME elliptical were enforced to determine the lifetime cycle, fatigue safety factor and fatigue damage on the femoral stem design [25,34].

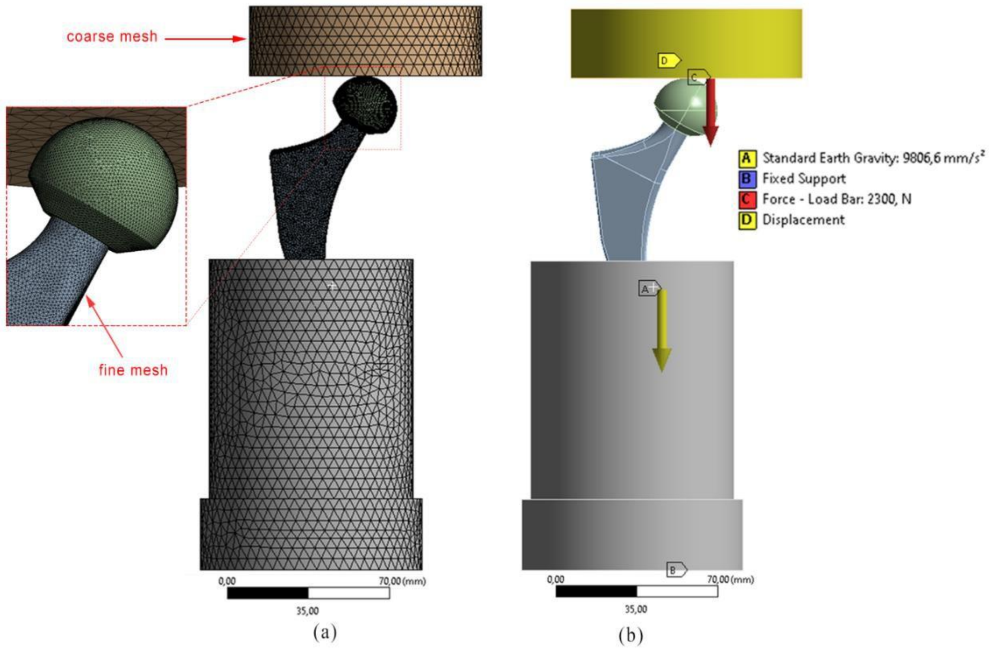

Fig 5. (a) Meshing finite element model of femoral stem ISO 7206 configuration, (b) Boundary condition finite element model of femoral stem ISO 7206 configuration.

3 Result & Discussion

<u>Experimental Fatigue Test</u>

Figure 6 shows the result of eight specimens Ti-6Al-7Nb as-cast endures the fatigue test. It is displayed that six specimens with the load cyclic 120% until 50% of yield strength underwent failure specimens at low cycles fatigue (LCF) with a fracture on the center diameter as presented sequentially.

The remaining two withstand specimens or “run-out” with a load range on 30% and 20% of yield strength (specimens C7 and C8) and reach the full set of high cycle fatigue (HCF) of 107 cycles. It shows that decreasing the amplitude stress can increase the fatigue cycle. The amplitude stress that the specimens can sustain through an infinitely large number of cycles with a 50% probability of failure was the criterion for the fatigue limit material [35]. Therefore, the fatigue limit of the Ti-6Al-7Nb as-cast was estimated in the range of 141 - 211 MPa due to the ability to withstand the maximum set cycle of the fatigue test, as illustrated in Figure 7.

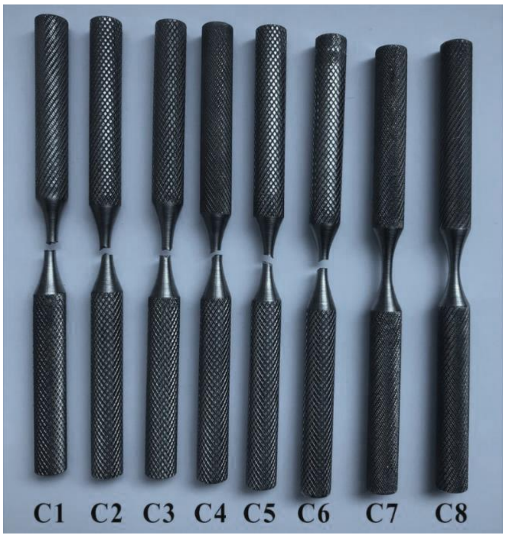

Fig 6. Condition of 8 specimens as-cast Ti-6Al-4V after undergoing the dynamic fatigue test.

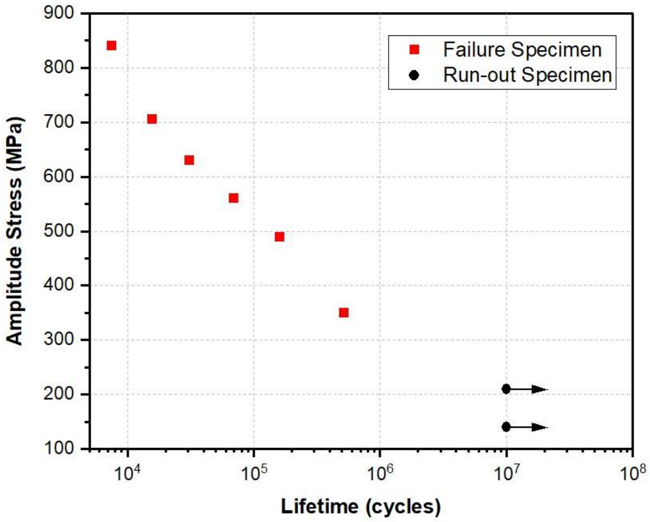

Fig 7. S-N fields of the Ti-6Al-7Nb as-cast with a total time of fatigue test was 580 hr.

A comparison of experimental fatigue on Ti alloy studied from earlier reports was collected in Figure 8 [36,37]. Those experimental fatigues employed the dynamic loading on axial condition R=-1, which is similar to this study. It was proved that the as-cast Ti-6Al-7Nb provides a similar range of fatigue limit with most of the fatigue as-cast examined previously to be around 140 – 220 MPa. On the other hand, hot-rolled and annealed Ti-6Al-7Nb perform the highest value of fatigue limit on 450 MPa rather than as-cast Ti alloys. It is known that the wrought specimens had a lower residual strain compared to the as-cast specimens. According to the examination of a single crystal and polycrystalline sample, the critical stress for slip has direct effect on characteristics of super- elasticity and it will be slightly affected by the number of grain boundaries [38].

The fatigue limit strength has a strong correlation with the tensile strength of the material as mentioned by Kasuga et al. on their previous study [39]. Thus, the fatigue ratio to the ultimate tensile strength ($\sigma_{limit}/\ \sigma_{uts}$) for those Ti alloys was calculated and compared in Figure 9, to exhibit the effect of tensile properties on the fatigue limit. As expected, hot-rolled and annealed

Ti-6Al-7Nb displayed the highest fatigue ratio and decrease in the sequence pointed out: Ti-5Al-13Ta, CP-Ti, Ti-6Al-7Nb, and Ti-6Al-4V as-cast alloys. In order to design the femoral stem component, it was recommended that the ratio of fatigue limit to ultimate tensile strength is 24%, using as-cast Ti-6Al-7Nb.

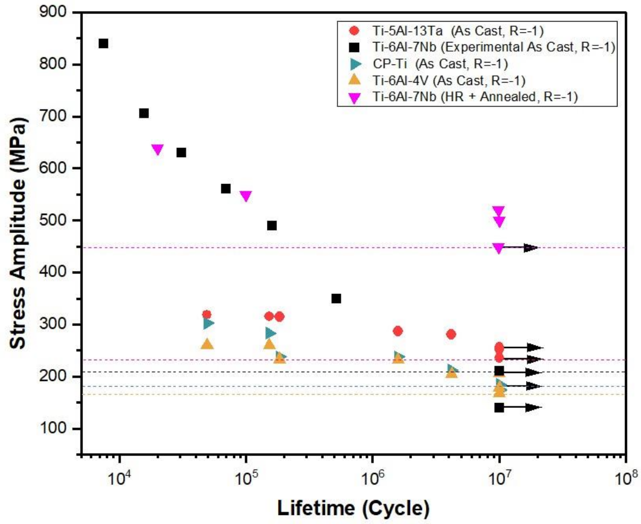

Fig 8. Comparison of S-N fields of Ti alloy for medical application from earlier reports.

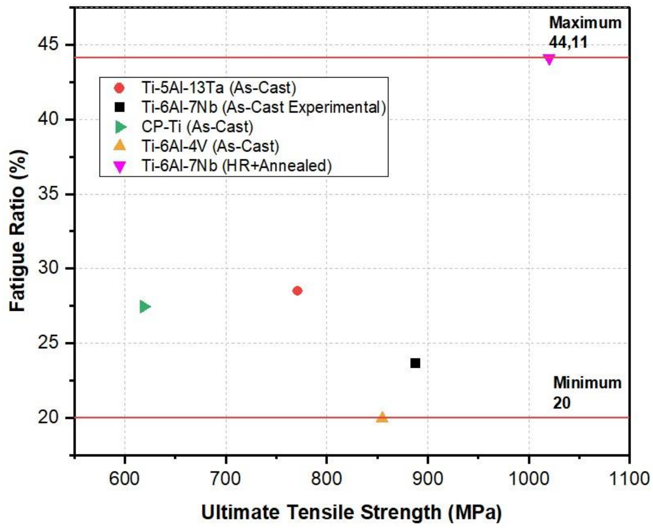

Fig 9. Comparison of fatigue ratio of Ti alloy for medical application from earlier reports.

ProFatigue Analysis

Figure 8 exposed some of the specimens stop logged fatigue cycles after achieving the maximum set cycles of 10 million, even without failure. As a consequence, it leads to an inaccurate estimation of the actual fatigue durability, which is somewhat essential for design and maintenance assessment [40]. Therefore, the ProFatigue program was implemented in this study to estimate the expected maximum failure cycles on fatigue limit with probabilistic modeling by Weibull distribution. S-N field data from 8 specimens of the Ti-6Al-7Nb as-cast was used as input the initial data for the probabilistic modeling on the ProFatigue program. The quantity of experimental data is sufficient to provide a reliable calculation, as mentioned in [19].

Figure 10, illustrated the calculation of normalized distribution, which enables entire S-N data inputs assumed to be associated with a single distribution which leads to a more precise estimation of the model parameters. The analytical formulation encompassing the entire S-N field could be known by combining the five estimated parameters [15]. The five model parameters generated are B = 0, C = 3.57, β = 2.42, λ = 27.49, and δ = 2.75, derived 49 numbers of iteration. Correspondingly, two run-out data emerged on probability failure (P_{fail}) of 0.5 with general normalized V around 30. It was indicated that the prediction of fatigue cycles was represented on the percentile curve of 50 %.

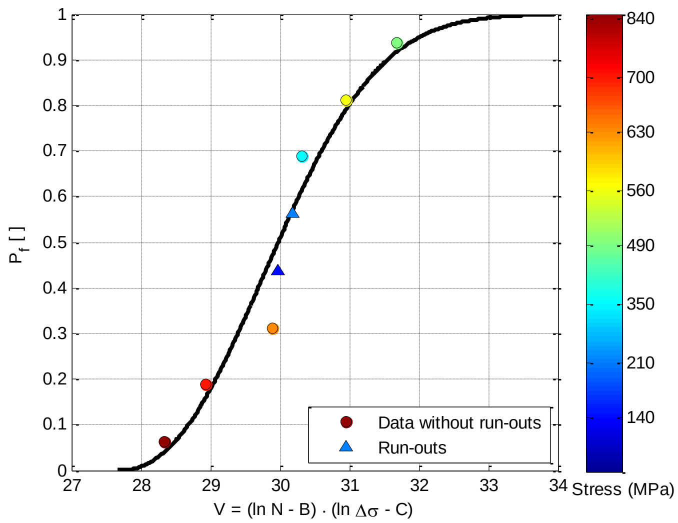

Fig 10. Cumulative distribution with five parameter functions.

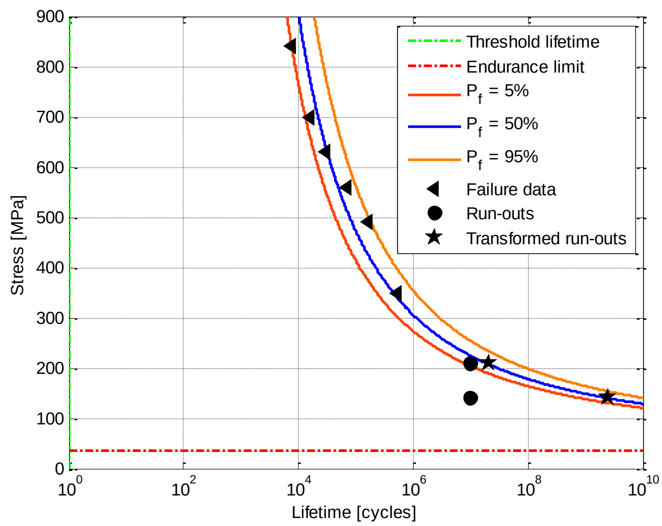

Fig 11. Estimation S-N curve with the new limit of failure cycles for two run-out data.

Percentile's curve established from hyperbolas sharing the asymptotes log N=B and log Δσ=C [40]. Probability failure curve with percentile of 5%, 50%, and 95% is shown in Figure 11. ProFatigue revealed two maximum cycles on fatigue limit data through a transformation of the run-out measurements into the failure cycle that corresponds to the mean curve P_{fail} 50%. As a result, the maximum failure cycle of run-out specimens Ti-6Al-7Nb as-cast was estimated at 2.144 x 107 and 2.823 x 109 cycles for stress amplitude 211 MPa and 141 MPa, respectively. Those very high cycle fatigue (VHCF) estimations play a role as a new limit of failure cycles material which would be applied in further observation on femoral stem design through the lifetime analysis in ANSYS based on the finite element analysis.

Post – Processing FEA

Investigation of the stress analysis and lifetime fatigue focused on femoral stem design under ISO 7206 standard was carried out completely through FEA. Implemented mechanical property of Ti-6Al-7Nb as-cast as mentioned in Table 1. The linear static analysis was conducted to figure out the stress distribution and total deformation occurring on the femoral stem design. The simulation's outcomes were visualized on various failure analyses with respective aims, including; von-mises stress, maximum principal stress, minimum principal stress, and total deformation showing in Figure 12.

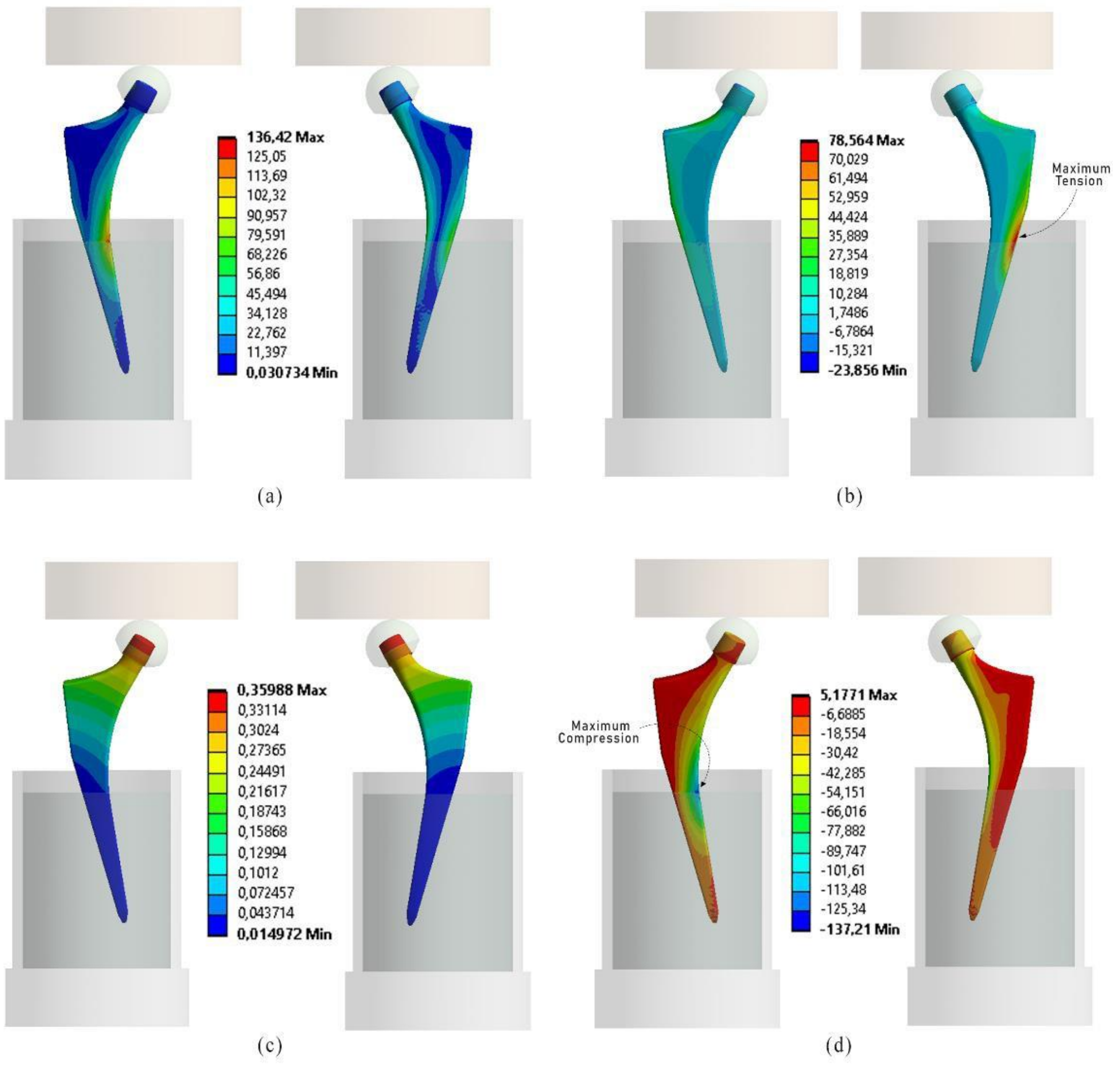

Fig 12. Two sides of FEA result on the designed femoral stem under ISO 7206 configuration on different failure analyses include: (a) von-mises equivalent stress, (b) maximum principal stress, (c) total deformation, and (d) minimum principal stress.

In Figure 12(a), von-mises stress resulted the maximum value of the resultant stress was 136.5 MPa which is lower than the fatigue limit of Ti-6Al-7Nb as-cast at 211 MPa. The location of maximum stress was on the medial region of the femoral stem and it displayed a similar location of maximum von-mises stress as reported previously [41-43]. The nonlinear contact between the femoral head and load bar allows a translation with small sliding interaction. It produces total deformation with a maximum value of 0,359 mm located on the top neck femoral stem, as presented in Figure 12(b). Furthermore, the maximum and minimum principal stress was employed to demonstrate the elements which experience absolute tensile and compressive stress, respectively. The result was shown that the reaction of axial -y force suppressed the femoral head causing the stress concentration on the interaction between the surface femoral stem and bone cement which acts as soft support, consequently the highest stress of compressive: -137,21 MPa and tensile: 78,56 MPa occur on the lateral anterior side and shaft distal of the femoral stem as illustrated on Figure 12(d, b). This phenomenon has been discussed in [21]. Additionally, that specific location of stress concentration has been evident as the crack initially in the actual experimental, as stated [44,45].

Therefore, the specific region observed in the lifetime analysis of femoral stem design. The number of cycles for material properties FE was inputted based on the S-N curve from the experimental fatigue test and Prod Fatigue estimation as shown in Figure 11. S-N curves parameters were attached to the FEA material database through determining the mean stress (σ_{mean}) and alternating stress ($\sigma_{alternating}$) on loading ratio R=-1, σ_{max} represents the maximum amplitude stress, and σ_{min} indicates the minimum amplitude stress, where ($\sigma_{max} = -\sigma_{min}$) is defined by the relation: [46]

$$\sigma_{mean} = \frac{\sigma_{max} + \sigma_{min}}{2} \tag{3}$$

$$\sigma_{alternating} = \frac{\sigma_{max} - \sigma_{min}}{2} \tag{4}$$

Investment casting would be selected as the manufacturing method of prototype femoral stems in future work; thus, it was essential to predict the porous possibilities that usually emerge in the casting process [47]. The porosity has a negative impact directly on the durability of the product [48]. In ANSYS, the fatigue strength factors meant a modification factor to the material properties that only affected the alternating stress [33]. Therefore, the fatigue strength factor settled at 0.7 to visualize the 30% porosity occurring on the femoral stem as studied [49]. The lifetime analysis has observed various failure theories utilize formulation as explained in Tabel 4. S_e represents the endurance limit, S_{ut} indicates a value of ultimate tensile strength, S_y expresses yield strength and N means the fatigue safety factors [34].

Table 4. Respective formulation of fatigue theories [34].

Fatigue theories	Formulation
Gerber	$\left(\frac{N.\sigma_a}{S_e}\right) + \left(\frac{N.\sigma_m}{S_{ut}}\right)^2 = 1$
Goodman	$\left(\frac{\sigma_a}{S_e}\right) + \left(\frac{\sigma_m}{S_{ut}}\right) = \frac{1}{N}$
Soderberg	$\left(\frac{\sigma_a}{S_e}\right) + \left(\frac{\sigma_m}{S_y}\right) = \frac{1}{N}$
ASME Elliptical	$\left(\frac{N.\sigma_a}{S_e}\right)^2 + \left(\frac{N.\sigma_m}{S_y}\right)^2 = 1$

According to ISO 7206 standard, the femoral stem should sustain on fatigue test with a minimum of 5 million cycles [24]. The capability of finite elements on fatigue prediction under ISO 7206 compared with the experimental study was well reported [9,50,51]. In this study, the fatigue theorizes of Gerber, Soderberg, Goodman, and ASME elliptic resulted in a similar calculation lifetime until 2.51 x 109 cycles the femoral stem could withstand the cyclic loading. It happened due to the stress level on principals stress and von-mises stress was maintained at a below level than the fatigue limit of the as-cast Ti-6Al-7Nb. The damage factor also exposed that the designed femoral has a factor of 0,398 in entire fatigue theories. The damage factors value under 1 means the design is in safe condition without failure until the lifetime is reached [33]. However, on the fatigue life safety factor, Gerber theories estimated slightly lower in 1,763 than Soderberg, Gerber and ASME elliptical was 1,791. All the fatigue theories calculate the safety factor value upper than 1, which indicates that the designed femoral stem could resist failure from cyclic loading [25].

CONCLUSION

In this study, the S-N curve data of as-cast Ti-6Al-7Nb was revealed experimentally. A comparison of the fatigue result shows that the fatigue limit on as-cast Ti-6Al-7Nb is 50% lower than wrought specimens of Ti-6Al-7Nb. It explains that the manufacturing method has a significant influence on the strength of material properties, which needs to be taken into consideration. The respective manufacturing method has its advantages and disadvantage related to the application.

ProFatigue software is proved to be an optimization instrument in observing exact failure cycles in the fatigue limit stress region based on Weibull regression modeling. According to the experimental fatigue data, the program has uncovered the estimation of maximum failure cycles on 140 MPa amplitude stress of as-cast Ti-6Al-7Nb at 2.823 x 109 cycles. Furthermore, it is beneficial to help the researcher in cost and time-efficiency in knowing the maximum failure cycles on various desired amplitude stress.

Static and fatigue behavior of designed femoral stem for Indonesian peoples was evaluated through the finite element analyses. Nonlinear contact and comprehensive parameters setting was implemented to approach the realistic condition. The femoral stem exhibited a low-stress concentration at the medial and distal regions, thus, resulted in high durability until 2.51 x 109 cycles, adequate to resist the cyclic loading without failure based on the lifetime analysis. It was evidenced computationally that material properties of as-cast Ti-6Al-7Nb are appropriate to implement in the femoral stem application due to it having fulfilled the required cycles on the endurance test according to ISO 7206 standard.

In conclusion, the outcome study convinced the possibility of investment casting as an alternative manufacturing method for a prototype of the designed femoral stem, as it is more well- established method and relatively cost-effective compared to other manufacturing process.

REFERENCES

[1] Ferry F.R. "Indonesia’s healthcare landscape: embracing innovation in the new health regime", Current Medical Research & Opinion 40 (6), pp. 1 – 8, **2024**. DOI: 10.1080/03007995.2024.2349732

[2] Department of Economic and Social Affairs, "Population and vital statistics report", United Nations, New York, United State, Series A, Vol. LXXIII, **2021**.

[3] Bajpai, A.K., Bajpai, J., Saini, R.K., Agrawal, P., Tiwari A. "Smart biomaterials devices, polymers in biomedical sciences", Taylor & Francis Group: CRC Press, pp. 1 – 2, **2016**. 978-ISBN: 1-4987-0698-8

[4] Varacallo, M., Herzog, L., Toossi, N., Johanson, N. "Ten-year trends and independent risk factors for unplanned readmission following elective total joint arthroplasty at a large urban academic hospital", The Journal of Arthroplasty 32, (6), pp. 1739 – 1746, **2016**. DOI: 10.1016/j.arth.2016.12.035

[5] Niinomi, M. "Mechanical biocompatibilities of titanium alloys for biomedical application", Journal of the Mechanical Behaviour of Biomedical Materials 1 (1), pp. 30 – 42, **2008**. DOI: 10.1016/j.jmbbm.2007.07.001

[6] Murr, L. E., et al. "Microstructure and mechanical behaviour of Ti–6Al–4V produced by rapid-layer manufacturing, for biomedical applications", Journal of the Mechanical Behaviour of Biomedical Materials 2 (1), pp. 20 – 32, **2009**. DOI: 10.1016/j.jmbbm.2008.05.004

[7] Skublova, L., Skorik, V., Mrazikova, R., Hadzima, B. "Corrosion resistance of Ti-6Al-4V titanium alloy with modified surfaces", Komunikacie 12, pp. 80 - 84, **2010**. DOI: 10.26552/com.C.2010.4.80-84

[8] Gallego, et al. "Microstructural characterization of Ti-6Al-7Nb alloy severe plastic deformation", Materials Research 5, pp. 786 – 791, **2012**. DOI: 10.1590/S1516-14392012005000100

[9] Okazaki, Y., Mori, J. "Mechanical performance of artificial hip stems manufactured by hot forging and selective laser melting using biocompatible Ti-15Zr-4Nb alloy", Materials MDPI 14, (4), pp. 732, **2021**. DOI: 10.3390/ma14040732

[10] Fellah, M., Assala, O., Labaïz, M., Dekhil, L., Iost, A. "Friction and wear behaviour of Ti-6Al-7Nb biomaterial alloy", Journal of Biomaterials and Nanobiotechnology 4 (1), pp. 374 – 384, **2013**. DOI: 10.4236/jbnb.2013.44047

[11] Lin, C.W., Ju, C.P., Chern Lin, J.H. "Comparison among mechanical properties of investment-cast c.p. Ti, Ti-6Al-7Nb and Ti-15Mo-1Bi alloys", Materials Transactions 45, (10), pp. 3028 – 3032, **2004**. DOI: 10.2320/matertrans.45.3028

[12] Koizumi, H., Ishii, T., Okazaki, T., Kaketani, M. "Castability and mechanical properties of Ti-15Mo-5Zr-3Al alloy in dental casting", Journal of Oral Science 60 (2), pp. 285 – 292, **2018**. DOI: 10.2334/josnusd.17-0280

[13] García-González, M. et al. "Optimized planning and evaluation of dental implant fatigue testing: a specific software application", Biology (Basel) 9 (11), pp. 372, **2020**. DOI: 10.3390/biology9110372

[14] Castillo, E. et al. "Specimen length effect on parameter estimation in modelling fatigue strenght by Weibull distribution", International Journal of Fatigue 28 (9), pp. 1047 – 1058, **2006**. DOI: 10.1016/j.ijfatigue.2005.11.006

[15] Fernández-Canteli, A., Przybilla, C., Nogal, M., López Aenlle, M., Castillo, E. "ProFatigue: a software program for probabilistic assessment of experimental fatigue data sets", Procedia Engineering, XVII International Colloquim on Mechanical Fatigue of Metals (ICMFM17) 74, pp. 236 – 241, **2014**. DOI: 10.1016/j.proeng.2014.06.255

[16] Castillo, E., Fernández-Canteli, A."A unified statistical methodology for modelling fatigue damage", 1st ed. Dordrecht Springer Netherlands, **2009**. ISBN: 978-1-4020-9181-0, DOI: 10.1007/978-1-4020-9182-7

[17] da Silva, L.F.R.C. "Monotonic and fatigue behaviour of double shear bolted joints: experimental and numerical studies", Master, Department of Engineering. University of Porto, **2020**.

[18] Muniz-Calvente, M., de Jesus, A.M.P, Correia, J.A.F.O., Fernández-Canteli, A. "A methodology for probabilistic prediction of fatigue crack initiation taking into account the scale effect", Engineering Fracture Mechanics 185, pp. 101 – 113, **2017**. DOI: 10.1016/j.engfracmech.2017.04.014

[19] Castillo, E., Muniz-Calvente, M., Fernández-Canteli, A., Blasón, S. "Fatigue assessment strategy using bayesian techniques", Materials 12, (9), pp. 3239, **2019**. DOI: 10.3390/ma12193239

[20] Bonfante, E. A., Coelho, P. G. "A critical perspective on mechanical testing of implants and prostheses", Advance in Dental Research 28 (1), pp. 18 – 27, **2016**. DOI: 10.1177.0022034515624445

[21] DePuy Synthes, "CORAIL hip system catalogue", Johnson & Johnson, France, **2016**.

[22] Safitri, P.N., et al. "Stem geometry recommendation for total hip replacement planning using computed tomography data analysis", Journal of Biomimetics, Biomaterials and Biomedical Engineering 55, pp. 23 – 34, **2022**. DOI: 10.4028/p-kz8jrp

[23] Qurashi, S., et al. "Stand up! Are normal weight-bearing forces sufficient for a 12/14 Morse taper locking in total hip arthroplasty? ", Hip International 32, (2), pp. 231 – 236, **2022**. DOI: 10.1177/1120700020967000

[24] International Standard, "Determination of endurance properties and performance of stemmed femoral components", Switzerland, ISO 7206-4, 3rd ed, **2010**.

[25] Zafer Senalp, A., Kayabasi, O., Kurtaran, H. "Static, dynamic and fatigue behaviour of newly designed stem shapes for hip prosthesis using finite element analysis", Material & Design 28 (5), pp. 1577 – 1583, **2007**. DOI: 10.1016/j.matdes.2006.02.015

[26] Lagoda, A., Nieslony, A. "Stress Analysis of Dental Implant Inserted in the Mandible", Strojnícky časopis – Journal of Mechanical Engineering 68 (1), pp. 25 – 32, **2018**. DOI: 10.2478/scjme-2018-0003

[27] Mahmoud, A., Wakabayashi, N., Takahashi, H., Ohyama, T. "Deflection fatigue of Ti-6Al-7Nb, Co-Cr, and gold alloy cast clasps", The Journal of Prosthetic Densitry 93 (2), pp. 183 – 188, **2005**. DOI: 10.1016/j.prosdent.2004.11.011

[28] Bousnane, T., Benbarek, S., Sahli, A., Serier, B., Bouiadjra, B.A.B. "Damage of the bone-cement interface in finite element analyses of cemented orhopaedic implants", Periodica Polytechnica, Mechanical Engineering 62 (2), pp. 173 – 178, **2018**. DOI: 10.3311/PPme.11851

[29] Babić, M., Verić, O., Božić, Ž., Sušić, A. "Finite element modelling and fatigue life assessment of a cemented total hip prosthesis based on 3D scanning", Engineering Failure Analysis 113, 104536, **2020**. DOI: 10.1016/j.engfailanal.2020.104536

[30] Jonathan, R.T.J., Browne, M., Lennon, A.B., Patrick, J.P., Taylor, M. "Cement mantle fatigue failure in total hip replacement: experimental and computational testing", Journal of Biomechanics 40 (7), pp. 1525 – 1533, **2006**. DOI: 10.1016/j.jbiomech.2006.07.029

[31] Šćepanović, M., et al. "Finite element analysis in defining the optimal shape and safety factor of retentive clasp arms of a removable partial denture", Vojnosanitetski pregled, Military-medical and pharmaceutical review 70 (11), pp. 999 – 1005, **2013**. DOI: 10.2298/VSP110526021S

[32] Heidi-Lynn, P., Bürgi, M., Wyss, Urs P. "Hip stem fatigue test prediction", International Journal of Fatigue 31 (5), pp. 894 – 905, **2009**. DOI: 10.1016/j.ijfatigue.2008.10.005

[33] Browell, R. "Calculating and displaying fatigue results on ANSYS", Development Engineer, ANSYS Inc, **2006**.

[34] Joshi, T., Sharma, R., Mittal, V.K., Gupta, V., Krishan, G. "Dynamic fatigue behaviour of hip joints under patient specific loadings", International Journal of Automotive and Mechanical Engineering 19 (3), pp. 10014 – 10027, **2022**. DOI: 0.15292/ijame.19.3. 2022.13.0773

[35] Taylor, L., and ASM international Handbook committee, "Metallography Structures and Phase Diagrams", Metals Handbook 8th ed. American Society for Metals, **1973**.

[36] Doi, H., Yoneyama, T., Kobayashi, E., Hanawa, T. "Fatigue property of Ti-5Al-13Ta Alloy Dental Castings in 0,9% NaCl Solution", Material Transactions 47 (9), pp. 2444 – 2447, **2006**. DOI: 10.2320/matertrans.47.2444

[37] Polyakova, V.V., Anumalasetty, V.N., Semenova, I.P., Valiev, R.Z. "Influence of UFG structure formation on mechanical and fatigue properties in Ti-6Al-7Nb alloy", In: IOP Conference series, Material Science and Engineering 6th International, France, pp 24, **2014**. DOI: 10.1088/1757-899X/63/1/012162.

[38] Nishijima, S. "Statistical analysis of fatigue test data", Journal of the Society Material Science Japan 29 (316), pp. 24 – 29, **1980**. DOI: 10.2472/jsms.29.24

[39] Kasuga, J., Yoneyama, T., Kobayashi, E., Hanawa, T., Doi, H. "Fatigue property of super-elastic Ti-Ni alloy dental casting", Materials Transactions 46 (7), pp. 1555 – 1563, **2005**. DOI: 10.2320/matertrans.46.1555

[40] Stanislav, S., Miarka, P., Sergio, B., Fernández-Canteli, A. "Evaluation of fatigue properties of S355 J2 and S355 J0 by using ProFatigue software", Mechanical Fatigue of Metals, Springer Nature Switzerland, pp. 213 – 219, **2019**. DOI: 10.1007/978-3-030-13980-3_28

[41] Giza, S., dos Santos, S.V., Ueki, M.M., Bertoni, F., Strohaecker, T.R. "Case study and analysis of fatigue failure in a THA stem", Engineering Failure Analysis 28, pp. 166 – 175, **2013**. DOI: 10.1016/j.engfailanal.2012.10.011

[42] Giza, S., et al. "Design aspects involved in a cemented THA stem failure case", Engineering Failure Analysis, 16 (1), pp. 512 – 520, **2009**. DOI: 10.1016/j.engfailanal.2008.06.016

[43] Guzmán, M.et al. "Finite element assessment of a hybrid proposal for hip Stem, from a standardized base and different activities", Applied Sciences 12 (16), pp. 7963, **2022**. DOI: 10.3390/app12167963

[44] Hernandez-Rodriguez, M.A.L., Ortega-Saenz, J.A., Contreras-Hernandez, G.R. "Failure analysis of a total hip prosthesis implanted in active patient", Journal of the Mechanical Behaviour of Biomedical Materials 3, (8), pp. 619 – 622, **2010**. DOI: 10.1016/j.jmbbm.2010.06.004

[45] Mierzejewska, Ż., Oksiuta, Z. "Failure analysis of a femoral hip stem made of stainless steel after a short time of exposure", Acta Mechanica et Automatica 8 (3), pp. 146 – 150, **2014**. DOI: 10.2478/ama-2014-0026

[46] Gedeon, M. "Mean stress and alternating stress", Technical TIDBITS Materion Brush Inc, 1, (63), **2014**. Available at: https://materion.de.com/-/media/files/alloy/newsletters/technical-tidbits/issue-no-63---mean-stress-and-alternating-stress.pdf [Accessed: 18 November 2022]

[47] Sutiyoko, S., Mahardika, M., Syamsudin, A. "Prediction of shrinkage porosity in femoral stem of titanium investment casting", Archives of Foundry Engineering. 16 (4), pp. 157 – 162, **2016**. DOI:10.1515/afe-2016-0102

[48] Leopold, G., Nadot, Y., Billaudeau, T., Mendez, J. "Influence of artificial and casting defects on fatigue strength of moulded components in Ti-6Al-4V alloy", Fatigue & Fracture of Engineering Material & Structure 38 (9), pp. 1026 – 1041, **2015**. DOI: 10.1111/ffe.12326

[49] Al Zoubi, N.F., Tarlochan, F., Mehboob, H. "Mechanical and fatigue behaviour of cellular structure Ti-6Al-4V alloy femoral stems: A finite element analysis", Applied Sciences 12 (9), pp. 4197, **2022**. DOI: 10.3390/app12094197

[50] Delikanli, Y.E., Kayacan, M.C. "Design, manufacture and fatigue analysis of lightweight hip implants", Journal of Applied Biomaterials & Functional Materials 17 (2), **2019**. DOI: 10.1177/228080019836830

[51] Taraka, H., Pardeep, P., Pankaj, B., Anilkumar, D., Indira, B., Aadarsh, K. "Friction stir welding tool life assessment through fatigue analysis", Strojnícky časopis – Journal of Mechanical Engineering 73 (2), pp. 163 – 180, **2023**. DOI: 10.2478/scjme-2023-0031